NASA CONTRACTOR REPORT

EXPERIMENTAL INVESTIGATIONS OF SOLID NITROGEN FORMED BY CRYOPUMPING

by K. W. Rogers

Prepared by
CELESTIAL RESEARCH CORPORATION
South Pasadena, Calif.
for

NATIONAL AERONAUTICS AND SPACE ADMINISTRATION • WASHINGTON, D. C. • AUGUST 1966

NASA CR-553

EXPERIMENTAL INVESTIGATIONS OF SOLID NITROGEN FORMED BY CRYOPUMPING

By K. W. Rogers

Prepared under Contract No. NASw-1282 by
CELESTIAL RESEARCH CORPORATION
South Pasadena, Calif.

for

NATIONAL AERONAUTICS AND SPACE ADMINISTRATION

For sale by the Clearinghouse for Federal Scientific and Technical Information
Springfield, Virginia 22151 – Price $2.00

ABSTRACT

An experimental investigation was made to determine the density, thermal conductivity and sticking coefficient of the nitrogen condensate formed on a cryopump. The cryopump temperature was in the range of 15^{o} to 26^{o}K and the incident gas temperature was 79^{o}K. Neither the density nor the thermal conductivity were significantly influenced by the deposition rate over the range of gas pressure ($2 \times 10^{-4} < P < 10^{-3}$ torr. The measured density was about .90 gm/cc and the measured thermal conductivity was about 1.2 mW/cm-^{o}K. The sticking coefficient varied with the cryopump temperature and the thickness of the condensate layer. The values of the sticking coefficient varied from about .85 to 1.0.

TABLE OF CONTENTS

LIST OF FIGURES

I. INTRODUCTION

The advent of large scale space chambers has brought about an increasing use of the cryopumping technique. In order to obtain the maximum utilization of the cryopumping technique it is necessary to determine its fundamental limitations. To determine these limitations the factors affecting the performance of the cryopump must be considered.

The measure of pump performance is the ratio of the net flux of molecules that are removed by the pump compared to the flux of molecules that strike the pump. In the case of the cryopump, this ratio is governed by (1) the vapor pressure of the condensate surface, which determines the rate at which molecules are released by the pump and (2) the sticking coefficient, which is the fraction of the incident molecules that are captured by the cryopump.

The vapor pressure of the surface is determined by the surface temperature of the condensate. This temperature depends upon the cryopanel temperature, the thermal conductivity of the condensate layer, the thickness of the condensate layer, and the heat flux. If the heat flux includes radiant energy it is necessary to consider the partial transparency of the condensate layer and account for the distribution of heat flux throughout the layer. The present study was concentrated on the case where the heat flux results from a gas condensation load thus the heat flux is introduced at the surface of the condensate layer and the surface temperature can be obtained from Eqn. (1).

$$T_c = \frac{q_c \Delta X_c}{k_c} + T_w \qquad (1)$$

T_c - condensate surface temperature
T_w - cryopump wall temperature

q_c - heat flux into condensate

ΔX_c - condensate thickness

k_c - condensate thermal conductivity

The vapor pressure of the condensate can be determined only if Eqn. (1) can be evaluated. The cryopump wall temperature can be measured and the heat flux (q_c) can be determined from the gas flux and the energy change required for condensation. The condensate thickness can be estimated if the time history of the mass flux is known.

$$\Delta X_c = \int_0^t \frac{\dot{m}_c}{\rho_c} \, dt \qquad (2)$$

$\dot{m}_c$ - mass flow condensation rate

ρ_c - condensate density

In order to solve Eqn. (2) it is necessary to know the condensate density as a function of deposition rate. The thermal conductivity must also be known as a function of deposition rate.

Since neither the condensate density nor the thermal conductivity has been carefully measured over a range of operating conditions, an investigation was made to determine the condensate density and thermal conductivity as a function of condensate deposition rate.

The other important parameter in determining the performance of a cryopump is the sticking coefficient. There have been significant differences in the experimentally determined values of the sticking coefficient. It is possible that the differences are due to the difficulty in maintaining an adequate calibration on the ionization gage and the mass flow meter. An investigation was made using an exponential pressure decay approach to avoid the necessity of a mass flow meter or an absolute

calibration on the ionization gage. These sticking coefficients were obtained over a range of condensate thicknesses and flow rates.

This report presents the results of these investigations of the condensate density, thermal conductivity and sticking coefficient.

II. FACILITY DESCRIPTION

2.1 Vacuum Chambers

All of the experiments were made in the facility shown in Figs. 1, 2, and 3. The outer chamber was a 23" x 31" cylinder which was pumped by a 4" diffusion pump. This chamber served as an insulating vacuum for the spherical test chamber and the 20 liter LN_2 reservoir.

The spherical test chamber was a spun copper sphere with a diameter of 30.5cm ($\pm$.3cm) and a wall thickness of .05cm. The spherical chamber temperature was held at 79°K ($\pm$ 1°) by the LN_2 system. By varying the pressure in the LN_2 reservoir, the LN_2 manifold was kept filled regardless of the LN_2 level in the reservoir. The circumferential variation of the wall temperature was estimated to be less than 2°K. The spherical chamber was connected to a small ambient temperature section which contained the view port, the pass-throughs, the pressure gages and the isolation valve. The vacuum isolation valve was open during pumpdown so the spherical chamber was evacuated by the outer chamber pumping system. When either cryopump was in operation the isolation valve was closed.

2.2 Gas Introduction System

The nitrogen gas that was to be cryopumped was obtained by vaporizing liquid nitrogen. The gas was stored in an 8 liter tank at a pressure of about 2 atmospheres. As the gas was removed by the cryopump, the tank pressure decreased. Changes in the tank pressure were measured with a

mercury manometer. The rate of gas flow into the spherical chamber was set by a variable leak valve.

The gas was introduced into the spherical chamber through the manifold shown in Fig. 2(a). This spherical array of .8cm copper tubes had 83 uniformly spaced orifices with a diameter of .061cm. The orifices were directed out toward the spherical chamber wall. It was calculated that this manifold system would assure that the variations in the gas flux to the cryopumps would be less than 1%.

2.3 Liquid Helium System

A 10 liter dewar of liquid helium was used to cool the cryopump. Instead of flowing helium through a transfer line into the chamber to cool the cryopump, a high purity (.99999+) copper rod was used to conduct the heat from the cryopump to the helium in the dewar. Since the cryopump was to be maintained in the range of 20°-30°K, it was more economical to use both the heat of vaporization of the helium (4.9 cal/gm) and the gas enthalpy between 4°K and 20°K (20 cal/gm). This was accomplished using the heat transfer line shown in Fig. 4.

In this arrangement, the heat from the cryopump and other sources was conducted down the copper rod. The rod was insulated from the LHe so the temperature difference between the copper rod and the LHe resulted in a heat flux through the smaller diameter brass rod at the bottom of the heat transfer line. This heat flux vaporized some LHe which then passed through the annulus between the copper rod and the 1.02cm stainless steel tubing.

Due to the high conductivity of the copper rod, the entire length of copper rod was at about 20°K. Since the gaseous helium entered at 4°K, there was a large initial temperature difference between the helium gas and the copper rod. This temperature difference in conjunction with the

high heat transfer coefficient of the small annulus caused most of the available enthalpy to be transferred from the helium to the copper bar and the gas left the annulus at nearly the temperature of the copper bar.

This heat transfer line has a major advantage over the alternative of using a conventional transfer line and regulating the flow rate to maintain the required temperature inasmuch as the heat transfer line is more nearly self-regulatory. For example if the heat load decreases, the conduction rod temperature also decreases which results in a decreased liquid helium boil-off rate. The fractional changes in boil-off rate and rod temperature are approximately $\frac{1}{2}$ the fractional change in heat flux.

On the other hand in a conventional gas transfer line with a fixed pressure drop the mass flow variation is always in the wrong direction and the constant pressure drop transfer line is unstable.

The temperature level of the copper rod could be varied by changing the length of the brass rod between the copper rod and the LHe. This was done by varying the length of teflon insulation that was mounted on the brass rod.

The temperature of the cryopump was set by varying the clamping force on the demountable coupling at the end of the copper rod. The conductance could be varied from 0 to .2 watt/^{o}K. This coupling also simplified installation since the heat transfer line was inserted in the dewar and the entire assembly was moved into place against the front flange of the outer vacuum chamber before the cryopump was coupled to the conduction bar.

In operation the heat transfer line was pre-cooled by LN_2, and upon insertion into the dewar, the rubber seal at the top of the dewar was quickly installed. This forced the vaporized helium to pass through the annulus during the cooldown. Some of the gas enthalpy was recovered and this procedure significantly reduced the LHe requirements during that phase of the operation.

III. DENSITY MEASUREMENT

3.1 Fundamental Approach

The density of the nitrogen condensate can be determined by first uniformly depositing a known quantity of gas on a cryopump of a known surface area and then measuring the thickness of the layer. The density can be obtained from Eqn. (3).

$$\rho_c = \frac{M_c}{A_c \, \Delta X_c} \tag{3}$$

M_c - mass of gas
A_c - condensate area

In order to use this approach it is necessary to accurately measure (1) the quantity of gas deposited (2) the cryopump surface area and (3) the thickness of the condensate layer.

The uniformity of the incident mass flux was assured by using the gas introduction system discussed in 2.2. The quantity of gas deposited was determined by using the 8 liter gas source and measuring the source pressure at the beginning of the run and at the end of the run.

The measurement of the surface area was facilitated by using a sphere for the cryopump. The cryopump is shown in Fig. 5. The cryopump

was a spun copper sphere with a diameter of 5.01cm ($\pm$.03cm) and a wall thickness of .07cm. The sphere was connected to the heat transfer line by a length of high purity copper rod. The sphere was supported from the spherical chamber by a stainless steel tube which also served as a pressure seal and a long heat conduction path. It was necessary to use a copper shield in order to prevent condensation on either the copper rod or the stainless support. This copper shield was fixed on the stainless steel support at a point where the temperature was too high for condensation. The copper shield did not extend to the cryopump, but left .09cm of the copper rod exposed. This exposed area was equal to the area lost from the sphere at the rod-sphere intersection so all calculations were based on the surface area of the sphere.

An analysis was made of the temperature gradient that would exist around the sphere. The temperature difference did not exceed .5^{o}K for the heat fluxes used during these tests (Q_{max} = 1 watt).

The thickness of the condensate layer was measured using the optical system discussed in the following section.

3.2 Experimental Apparatus

The thickness of the condensate layer was measured using the optical system shown in Fig. 6. The 20 power telescope was aligned and fixed in place with the vertical cross hair nearly tangent to the cryopump surface. By rotating the optical flat, the light rays were deflected to bring the vertical cross hair tangent to the sphere. As the condensate layer was being formed, the optical flat was rotated to maintain the vertical cross hair tangent to the surface. The relationship between angular rotation of the optical flat as shown by the pointer and the linear distance at the surface of the sphere was obtained by a calibration. Since the optical system was nonlinear, a calibrated scale was used with

the pointer to facilitate data read out. This system had a useful range of about $\pm$.5cm and an accuracy of about $\pm$.003cm. This distance (.003cm) corresponded to a pointer displacement of .2cm. The necessary light source was obtained by using a simple convex lens with a small high intensity lamp.

The temperature of the cryopump was measured using a gold-2.1 at.% cobalt versus chromel thermocouple. The thermocouple was potted in a .6cm diameter copper tube that was flush mounted on the spherical cryopump. The thermocouple was referenced to the wall of the spherical chamber where the junctions were formed with .025cm constantan wires which were used as leads to the voltmeter. The temperature of the spherical chamber wall was found to be 78.5^{o}K at the reference point. The output of the thermocouple was measured using a Hewlett-Packard 419A D.C. voltmeter.

A check calibration was made using liquid helium (4.2^{o}), a solid nitrogen bath (53.1^{o}) and an ice bath (273^{o}) with a liquid nitrogen reference (77.4^{o}). The thermocouple output was consistently 5% greater than the values given by the N.B.S. so a 5% correction was used throughout the data reduction.

3.3 Test Procedure

In a typical test, the spherical chamber was pumped to about 10^{-5} torr through the isolation valve. The isolation valve was then closed and the spherical cryopump was cooled by tightening the coupling on the heat transfer line. When the temperature stabilized the chamber pressure read about 2×10^{-6} torr. This was the result of outgassing in the warm section that contained the gage, and did not reflect the pressure in the chamber.

The optical system was used to establish the zero reference for the condensate layer. The moveable thermocouple used in the thermal conductivity tests was left in one position during the time the condensate was being deposited. The optical system was used with this thermocouple to verify that there was no relative motion between the spherical cryopump and the telescope during the testing.

After the pressure in the source volume was recorded the variable leak valve was adjusted to maintain a specified chamber pressure during the deposition period. The position of the condensate layer and the pressure in the source volume were recorded periodically throughout the run. To avoid local heating of the condensate layer, the light source was on only during the brief measurement periods.

The level of noncondensable gas pressure was checked approximately four times during each run. This was done by shutting off the flow into the chamber, and observing the chamber pressure. This pressure did not exceed 10% of the chamber pressure. These noncondensable gases were vented into the outer chamber by opening the isolation valve for about 15 sec. An insignificant quantity of gas was cryopumped during this venting operation.

At the completion of the run, the flow was shut off and a final set of measurements were taken before proceeding with the thermal conductivity experiments.

3.4 Test Results

The variation of the condensate thickness and the mass of condensate with time is presented in Fig. 7 for a run that was made with an indicated pressure of about 10^{-3} torr and a cryopump temperature of $25^{\circ}K \pm 1^{\circ}$. When allowance is made for the thermal transpiration, the pressure of the gas in the chamber is estimated to be 5×10^{-4} torr.

The free molecular flow mass flux was calculated assuming a unity sticking coefficient. Fig. 7 shows that while the experimental mass flux was essentially constant during the run, it exceeded the free molecular flow value. The flow was not free molecular since the mean free path of the molecules was about 1/3 the diameter of the cryopump. The mean free path being comparable to the cryopump diameter resulted in a directed mass motion toward the pump which increased the mass flow beyond the free molecular flow value.

The data from Fig. 7 has been replotted in Fig. 8 to show the variation of condensate thickness with mass of gas condensed. The linear relationship between the two indicates the density of the condensate did not vary during the run.

The density was calculated using the slope ($\Delta M/\Delta X_c$) obtained from Fig. 8. The cryopump area was corrected for the thickness of the condensate layer. The resulting value of the density was .90 gm/cc. $\pm 5\%$.

The accuracy of the data was estimated from the summation of the possible errors in the terms M_c, A_c and ΔX_c. The uncertainties in M_c and A_c were estimated to be 1.5%. A 2% uncertainty in the term ΔX_c was the result of the $\pm$.003cm accuracy of the optical system.

Figs. 9 and 10 show the corresponding data for a run made with a nominal indicated pressure of 2×10^{-4} torr and a cryopump temperature of $26^{\circ}K \pm 1^{\circ}$. When allowance is made for thermal transpiration the chamber pressure becomes about 10^{-4} torr. It is apparent from Fig. 9 that the mass flow increased with time, and the experimental mass flow rate is above the theoretical value. While both of these discrepancies may have resulted from maintaining a nominal 2×10^{-4} torr, it is probable that there was still some directed mass motion since the mean free path was only about a factor of two greater than the diameter of the cryopump.

The density was calculated to be .90 gm/cc $\pm$ 6½%. The increased uncertainty was due to the thinner condensate layer.

It is apparent that to the accuracy of these experiments the condensate density was not a function of the deposition rate. The condensate density is about 88% of the density of solid nitrogen formed from the liquid state (ρ = 1.02 gm/cc).

IV. THERMAL CONDUCTIVITY MEASUREMENT

4.1 Fundamental Approach

The thermal conductivity of the condensate was determined from the fundamental equation of heat conduction.

$$q_c = k_c \left(\frac{d T}{d X}\right)_c \tag{4}$$

By assuming neither the conductivity nor the elemental area changed across the distance ΔX, Eqn. (4) could be solved for k_c.

$$k_c = q_c \frac{\Delta X_c}{\Delta T_c} \tag{5}$$

The thermal conductivity of the condensate could be determined if a known heat flux was established through a condensate layer of known thickness and if the temperature change through the condensate was measured.

A condensate layer of known thickness was obtained by using the layer formed on the 5cm sphere during the density measuring experiments.

A heat flux was established by introducing enough helium to maintain gaseous conduction between the spherical chamber and the spherical cryopump. The helium pressure level was a compromise between a lower pressure which would minimize convective heat transfer, and a higher pressure which

would both increase the heat transfer rate to the thermocouples and reduce the temperature jump at the surface of the condensate. The pressure was high enough (.3 torr) to cause some convection so the heat flux in the helium could not be calculated from the conduction equation for spherical surfaces.

Convective heat transfer measurements of previous investigators have had large percentages of uncertainty so it was necessary to determine the heat flux during the course of the experiments. This was done by measuring the helium temperature in the vicinity of the cryopump wall and calculating the heat flux from Eqn. (6).

$$q_c = q_{He} = k_{He} \left(\frac{d\,T}{d\,X}\right)_{surface} \qquad (6)$$

The surface temperature of the condensate was obtained by extrapolating the measured helium gas temperature to the surface of the condensate. The temperature of the condensate at the cryopump interface was assumed equal to the cryopump temperature which was constant during a run. In the measurements, a single moveable thermocouple was used to determine the difference between the helium gas temperature and the cryopump temperature. The use of a single thermocouple eliminated errors due to variations between thermocouples, and the direct measurement of a temperature difference instead of two temperatures removed the necessity of working with the difference between large numbers.

This procedure still contained errors due to temperature jump and inadequate thermal isolation of the thermocouple. The temperature jump error results from extrapolating the helium temperature gradient to the surface wince kinetic theory shows that the apparent gradient within one or two mean free path lengths of the surface is quite different from the continuum gradient. The thermal isolation errors result from heat conduction along the wires which causes the thermocouple to indicate a temperature different from that of the medium surrounding the junction.

These errors were eliminated by making a tare calibration near the beginning of each run. In this tare calibration a helium temperature profile was obtained after enough condensate was deposited to assure that the surface interaction would be representative of a helium-condensate interaction instead of a helium-copper interaction. The condensate layer was still thin enough to minimize the correction that was required for the temperature change through the condensate layer. This tare calibration was then used as a reference for the final helium temperature profile and the value of ΔT_c was obtained from the difference of these curves.

4.2 Experimental Equipment

The spherical cryopump described in the section on density measurement was used in this phase of the experiments.

The moveable thermocouple was mounted on the cryopump as shown in Fig. 11. The position of the thermocouple was varied by moving a bell crank that was attached to a rotary pass-through. The thermocouple could be positioned to within $\pm$.005cm of the desired location. The position of the thermocouple was determined using the optical system previously discussed. The thermocouple was gold - 2.1 at.% cobalt versus chromel and was similar to the one described in the section on density measurement. The wires had been butt welded so that junction dimensions were comparable to those of the wire (d = .0127cm). A check calibration showed that this method of forming the junction produced a thermocouple with the same output as those formed by soldering. The thermocouple was referenced to the spherical cryopump where the junctions were formed with .025cm constantan wires which were used as leads to the voltmeter. The thermocouple output was measured using a Hewlett-Packard 419A D.C. voltmeter.

The length of thermocouple wire between the support and the thermocouple junction was sufficient to prevent the support temperature

from influencing the temperature of the thermocouple junction, however, since the gas isotherms were spherical surfaces, the thermocouple was in a varying temperature field. This elevated the temperature of the junction about .5°K.

4.2 Test Procedure

The thermal conductivity tests were run concurrently with the density measurements and the procedures for forming a condensate layer are given in Section 3.3.

After a condensate layer with a thickness of about .005cm was formed, the nitrogen flow was stopped so the tare temperature profile could be obtained. This profile was used as a reference level. The heat flux for this procedure was established by introducing helium into the spherical chamber through the inlet manifold. The pressure was monitored on a Pirani gage. Once conditions were stabilized, a temperature profile was obtained for the region within .2cm from the surface of the condensate. The helium was then pumped out and the nitrogen flow was re-established.

When the density measurement was completed, the helium was again introduced and the final temperature profile was obtained.

4.4 Test Results

The helium temperature profiles that were obtained for several exploratory configurations are presented in Fig. 12. Before considering the details of the configurations some general features should be discussed.

The data show the same spatial resolution obtained during the density measurements - $\pm$.003cm. The temperature data appear to have a scatter of about .1°K. At temperature differences below 2°K this scatter

is due to the error in spatial resolution since the percentage error in the voltmeter system did not exceed 6%.

It is apparent that there was a zero shift since the data show the thermocouple temperature is below the cryopump temperature. Calculations show that the error is in the measurement of the cryopump temperature and it is due to heat conduction along the thermocouple wires. This conduction is the result of the high temperature gradients ($50^{o}K/cm$) in the helium near the surface of the cryopump.

There is a further uncertainty introduced by the finite size of the thermocouple wire. The temperature varies about $.5^{o}K$ over the width of the thermocouple wire.

While these problems make it difficult to specify the temperature level of the experiment and account for the bulk of the uncertainty of the temperature of the cryopump, they do not significantly influence the accuracy of either the helium temperature gradient or the condensate temperature change. Thus the data is satisfactory since these are the important terms in calculating the thermal conductivity of the condensate.

The helium temperature profiles that are presented in Fig. 12 were taken to investigate the effects of surface conditions and helium pressure level. The effects of surface conditions are negligible as far as this investigation is concerned since there is no discernible difference between the data taken with a clean surface and that taken with a .005cm condensate layer. The effects of helium pressure variations were also small since varying the pressure by .1 torr only changed the temperature level by $.2^{o}K$. The variations of helium pressure experienced during testing were about $\pm$.01 torr, so the temperature error due to this source was negligible.

Fig. 13 shows a comparison of the helium temperature profiles obtained from a tare run with a .005cm condensate layer and from a final run with a .145cm layer. During deposition the pressure of the $79^{o}K$ gas was estimated to be 5.2×10^{-4} torr.

This data shows that the temperature change through the condensate layer (ΔT_c) is $1.5^{o}K$.

Included on the plot are the theoretical temperature profiles for conduction between the cryopump and the spherical chamber. In obtaining the theoretical profiles it was necessary to consider the temperature dependency of the thermal conductivity of the helium. It was found that the conductivity values presented in Ref. (1) and Ref. (2) were within $\pm 1\%$ of Eqn. (7). ($20^{o}K < T_{He} < 100^{o}K$.)

$$k_{He} = 3.72 \times 10^{-5} T^{.652} \text{ watt/cm}^{o}\text{K} \qquad (7)$$

The heat flux at the surface of a sphere with a radius (r_c) is given by Eqn. (8).

$$q = 2.25 \times 10^{-5} \frac{T_\infty^{1.656} - T_c^{1.652}}{r_c (1 - r_c/r_\infty)} \quad \text{watt/cm}^2 \qquad (8)$$

r_∞ - radius of outer sphere
T_∞ - temperature of outer sphere

The resultant temperature profile was obtained from Eqn. (9).

$$T = T_c \left[1 + \frac{\left(T_\infty/T_c\right)^{1.652} - 1}{1 + r_c/r_\infty} \frac{\Delta r/r_c}{(1 + \Delta r/r_c)^3} \right]^{\frac{1}{1.652}} \qquad (9)$$

T = temperature at the radial distance $r_c + \Delta r$

The profiles obtained from Eqn. (9) have the same shape as the experimental ones, but the experimental slope is steeper. The steeper experimental slope is the result of convection since the increased heat flux due to convection must appear as an increased temperature gradient at the wall. It is clear from Fig. 13 that when the theoretical curves are multiplied by arbitrary constants they are in excellent agreement with the experiments. These arbitrary constants indicate the increase in heat flux due to convection (10-15%).

The heat flux at the surface was calculated by multiplying the theoretical flux by 1.15. The thermal conductivity of the condensate was calculated by evaluating Eqn. (5).

$$k_c = q_c \frac{\Delta X_c}{\Delta T_c} = (1.15)(.0119)\frac{.145}{1.5} = 1.32 \times 10^{-3} \pm 13\% \text{ watt/cm}^{\circ}\text{K} \quad (10)$$

The accuracy of the data was obtained by summing the possible errors in the terms q_c, ΔX_c and ΔT_c. The possible error in q_c included 1% from Eqn. (7) for the helium conductivity, 1% for the curve fitting between the theoretical and experimental temperature profiles and 2.5% for the error in experimental slope which results from the 1° uncertainty in temperature level. This latter term is caused by the temperature dependency of the thermoelectric power of the thermocouples. The total possible error for q_c was 4.5%. The possible error for ΔX_c was discussed in the section on density measurements and was 2%. The possible error for ΔT_c was estimated to be $.1^{\circ}$K or 6.5%. The sum of these uncertainties is 13%.

A similar set of data was obtained for the condensate that was deposited at a gas pressure of 10^{-4} torr- this data is presented in Fig. 14. Except for more scatter in the tare run, the data is similar to that in Fig. 13. A comparable procedure was used to obtain the thermal conductivity of the condensate.

$$k_c = 1.11\ (.0118)\ \frac{.082}{.95} = 1.13 \times 10^{-3} \pm 17.5\%\ \text{watt/cm}^{\circ}\text{K} \quad (11)$$

The increased uncertainty results from the thinner condensate layer used in the experiments.

While Eqns. (10) and (11) show a change in thermal conductivity with deposition rate, the difference is within the experimental accuracy of the data so it is concluded that there was no significant change in thermal conductivity over the range of conditions tested.

Investigations of the thermal conductivity of solid nitrogen were reported in Ref. (3) and Ref. (4). The nitrogen layer used in Ref. (3) was obtained by cryopumping at a gas pressure in the range .01-.1 torr. The resulting thermal conductivity ($k = 1.02 \times 10^{-3}$ watt/cm$^{\circ}$K) was comparable to that attained in the present investigation.

In Ref. (4) the layer was formed by solidifying liquid nitrogen. The values of thermal conductivity obtained during that investigation are compared with those of the present investigation in Fig. 15. The values of thermal conductivity obtained in Ref. (4) were a factor of 3 greater than those of the present investigation. This is in contrast to the density investigation where it was found that the method of forming the solid had only a small influence. Apparently the 12% voids that are contained in the solid formed by cryopumping result in a large resistence to heat flow and the thermal conductivity is reduced by a factor of 3.

V. STICKING COEFFICIENT MEASUREMENT

5.1 Fundamental Approach

There have been several previous investigations of the sticking coefficient. In general these investigations were made using the dynamic flow approach. In this approach the sticking coefficient is calculated from measurements of the net mass flux to the cryopump and the gas density in the chamber. Assuming the gas density is low enough for free molecular flow conditions to exist, the net mass flux is given by Eqn. (12).

$$\dot{m}_{net} = \sigma_\infty n_\infty \bar{v}_\infty/4 - \sigma_c n_c \bar{v}_c/4 \qquad (12)$$

σ - sticking coefficient
n - gas density
$\bar{v}$ - mean molecular speed

subscript
∞ - chamber conditions
c - condensate surface

The term involving n_c is the molecular flux due to the vapor pressure of the condensate surface, and σ_c is the corresponding sticking coefficient which is probably unity for these conditions.

Eqn. (12) can be solved for the sticking coefficient.

$$\sigma_\infty = \frac{\dot{m}_{net} + \sigma_c n_c \bar{v}_c/4}{n_\infty \bar{v}_\infty/4} \qquad (13)$$

Now even if the vapor pressure is negligible, this calculation of the sticking coefficient still depends upon an accurate determination of both the mass flow rate and the density of the gas in the chamber. The average molecular speed must also be determined, but usually this can be done quite accurately. Absolute values of mass flow rate and density are difficult to measure at the rarefied conditions found in vacuum chambers and it seems possible that this accounts for the disagreement between different investigations.

These problems were avoided in the present investigation by using the cryopump to remove the gas from a chamber of known volume. The variation of the chamber density with time can be obtained by using Eqn. (14).

$$\dot{m}_{net} = - \frac{V_\infty}{A_c} \frac{d\, n_\infty}{d\, t} = \sigma_\infty\, n_\infty\, \bar{v}_\infty/4 - \sigma_c\, n_c\, \bar{v}_c/4 \qquad (14)$$

Most previous investigators have found that the variation of σ_∞ with density is negligible. If the surface temperature is constant, then n_c does not vary and Eqn. (14) can be integrated.

$$\frac{n_\infty - (\sigma_c/\sigma_\infty)\, n_c (\bar{v}_c/\bar{v}_\infty)}{n_{\infty_o} - (\sigma_c/\sigma_\infty)\, n_c (\bar{v}_c/\bar{v}_\infty)} = \exp - \sigma_\infty \frac{A_c}{V_\infty} \frac{\bar{v}_\infty}{4}\, t \qquad (15)$$

n_{∞_o} = density when pumping started ($t = 0$)

Eqn. (15) shows that in the limiting case when the vapor pressure term is negligible it is not necessary to determine the absolute value of the density. Only the density ratio, the gas temperature and the geometric sizes must be known to compute the sticking coefficient from the pumpdown data. Thus instead of requiring that the ionization gage retain its calibration during the test, it is only required that the slope of the output versus density does not change. This approach has the further advantage of eliminating the mass flow metering system.

Even in the case where either the vapor pressure or the outgassing rate is not negligible, the absolute level of the calibration is not important if the ionization gage remains linear since the gage sensitivity cancels out in the ratio of the densities.

In order to apply this approach it is necessary to either fill the chamber to a preselected density and then initiate the cryopumping, or establish a steady flow rate with the cryopump in operation and then abruptly stop the inflow. The latter approach was used in these tests.

5.2 Experimental Equipment

In this phase of the test, a disc cryopump was mounted in the spherical chamber. The cryopump is shown schematically in Fig. 16.

A small fast acting valve was installed in the gas inlet piping to allow an abrupt cut off of the inflow.

The pressure decay was measured using a CVC GIC-111 ionization gage system. The output from the controller was used as input to a Moseley 7000A x,y plotter. The plotter was used with a time sweep on the x axis and the ionization gage output on the y axis. The linearity of the plotter was specified as .1% of the full scale.

5.3 Test Procedure

During a typical test sequence, the heat transfer coupling was loosened and the disc cryopump temperature rose to 35^{o}-40^{o}K. After all of the nitrogen had been evaporated and pumped out into the cylindrical chamber the isolation valve was closed and the coupling was adjusted to maintain the cryopump termperature. The fast acting valve was opened and the metering valve was used to set the pressure level in the chamber. When the required quantity of gas had been deposited the recorder was turned on and the fast acting valve closed. At the end of the pumpdown, either the flow was re-established for another run or the cryopump was warmed up to remove the condensate layer.

5.4 Test Results

A typical trace of the variation of pressure with time is shown in Fig. 17. The trace differs from an exponential pumpdown during the first few seconds because there was a quantity of gas contained in the inlet manifold system which continued to supply gas to the chamber after the fast acting valve was closed. A theoretical analysis was made of this flow system. It was found that the form of Eqn. (15) was still valid after the initial transient. The level of the density ratio was increased, but the term $\exp - \sigma_{\infty} (A_c/V_{\infty})(\bar{v}_{\infty}/4)t$ was not changed.

The minimum pressure indication was in the range of $2 - 5 \times 10^{-6}$ torr. This level was set by outgassing in the warm (300^{o}K) section containing the ionization gage and was not representative of the pressure level in the spherical chamber, however the minimum pressure must be used as a zero reference in evaluating the pumpdown curves. This is illustrated in Fig. 18 which shows the pumpdown of Fig. 17 on a semi-logarithmic plot. In order to obtain a logarithmic decay it was generally necessary to use a zero reference pressure that was about $4 - 8 \times 10^{-7}$ torr greater than

the minimum pressure. It appears that the pumpdown curves were characterized by a logarithmic decay to this increased zero reference pressure level followed by a slower decay to the final pressure level. The slower decay may have been due to the finite term required for the adcorption-desorption equilibrium to be re-established at the new pressure level.

The term $\sigma_\infty (A_c/V_\infty) \bar{v}_\infty/4$ was determined graphically by plotting the data as shown in Fig. 18. The sticking coefficient was then calculated by using the appropriate values of A_c, V_∞ and $\bar{v}_\infty$. In calculating the area of the cryopump it was assumed that the molecules entering the .017cm gap between the cryopump and the shield would be captured before they could return to the chamber. The exponential term was calculated to be .209 σ_∞/sec so a 10% change in σ_∞ caused about a one second change in the time required for the pressure to change a decade. It was generally found that the graphical solution of the time required for a decade change was accurate to about $\pm$.2 sec.

Data was obtained for a range of initial chamber pressure, cryopump temperature and condensate thickness. Most of the data was taken with an initial pressure of 10×10^{-5} torr. The data taken at 10^{-4} torr and 10^{-6} torr was of limited accuracy however, the sticking coefficient appeared to be independent of pressure.

The variation of sticking coefficient with cryopump temperature is shown in Fig. 19. The uncertainty in the level of the data is estimated to be $\pm$8%. This resulted from a summation of the following error terms; cryopump area 2%, time from the graphical solution 2%, chamber volume 1%, ionization gage nonlinearity 2½% and mean velocity ½%.

Data from Ref. (5) is included on the plot. The sets of data show a similar trend but the levels are different.

The variation of sticking coefficient with thickness of condensate layer is shown in Fig. 20. It was found that the sticking coefficient increased about 6% as the thickness of the condensate layer was increased

from 0 to .008cm. Further increases in thickness did not change the sticking coefficient. This is in qualitative agreement with the results reported in Ref. (6) when it was found that the sticking coefficient of CO_2 on a LN_2 cooled cryopump increased 30% over a similar range of condensate layer increase.

The sticking coefficients shown in Fig. 20 exceed unity which is the maximum theoretical value, however the difference is within the limits of the accuracy of the data.

The condensate thickness investigation was only made at 17.5°K but if it is assumed that the influence is independent of temperature, the data shown in Fig. 19 should be uniformly increased 6% to correspond to the data of Ref. (5) which was obtained with a previously deposited layer of condensate. This further increases the difference between the two sets of data.

VI. CONCLUSIONS

The density of solid nitrogen condensate obtained by cryopumping 79°K nitrogen gas was independent of the gas pressure in the range of $2 \times 10^{-4} < P < 10^{-3}$ torr. The density of the condensate was .90 gm/cc which is about 88% of the density of solid nitrogen formed from liquid nitrogen. The thermal conductivity of the condensate was independent of the deposition rate over the same pressure range. The thermal conductivity was approximately 1.2 mW/cm°K which is about one-third the value obtained for solid nitrogen formed from liquid nitrogen.

The sticking coefficient for the 79°K nitrogen gas was a function of the cryopump temperature and the thickness of the condensate layer if the layer was less than .0008cm thick. The values of the sticking coefficient ranged from about .85 to 1.0.

REFERENCES

1. " A Compendium of the Properties of Materials at Low Temperature (Phase I)", WADD Technical Report 60-56, October 1960.

2. " Argon Helium and the Rare Gases", Vol. I, Interscience Publishers, Inc. 1961.

3. Krishnamurty Karamcheti, " A Note on the Thermal Conductivity of Solid Nitrogen and the Direct Condensation of Nitrogen Gas Into a Solid", USCEC Rept 56-206, January 1959.

4. Roder, H. M., " The Thermal Conductivity of Solid Nitrogen", Cryogenics, Vol. 2, No. 5, September 1962.

5. Dawson, J. P., " Prediction of Cryopumping Speeds in Space Simulation Chambers", AIAA Space Simulation Testing Conference, November 1964.

6. Wang, E.S.J., Collins, Jr., J.A. and Haygood, J. D., "General Cryopumping Study", Advances in Cryogenic Engineering, Vol. 7, August 1961.

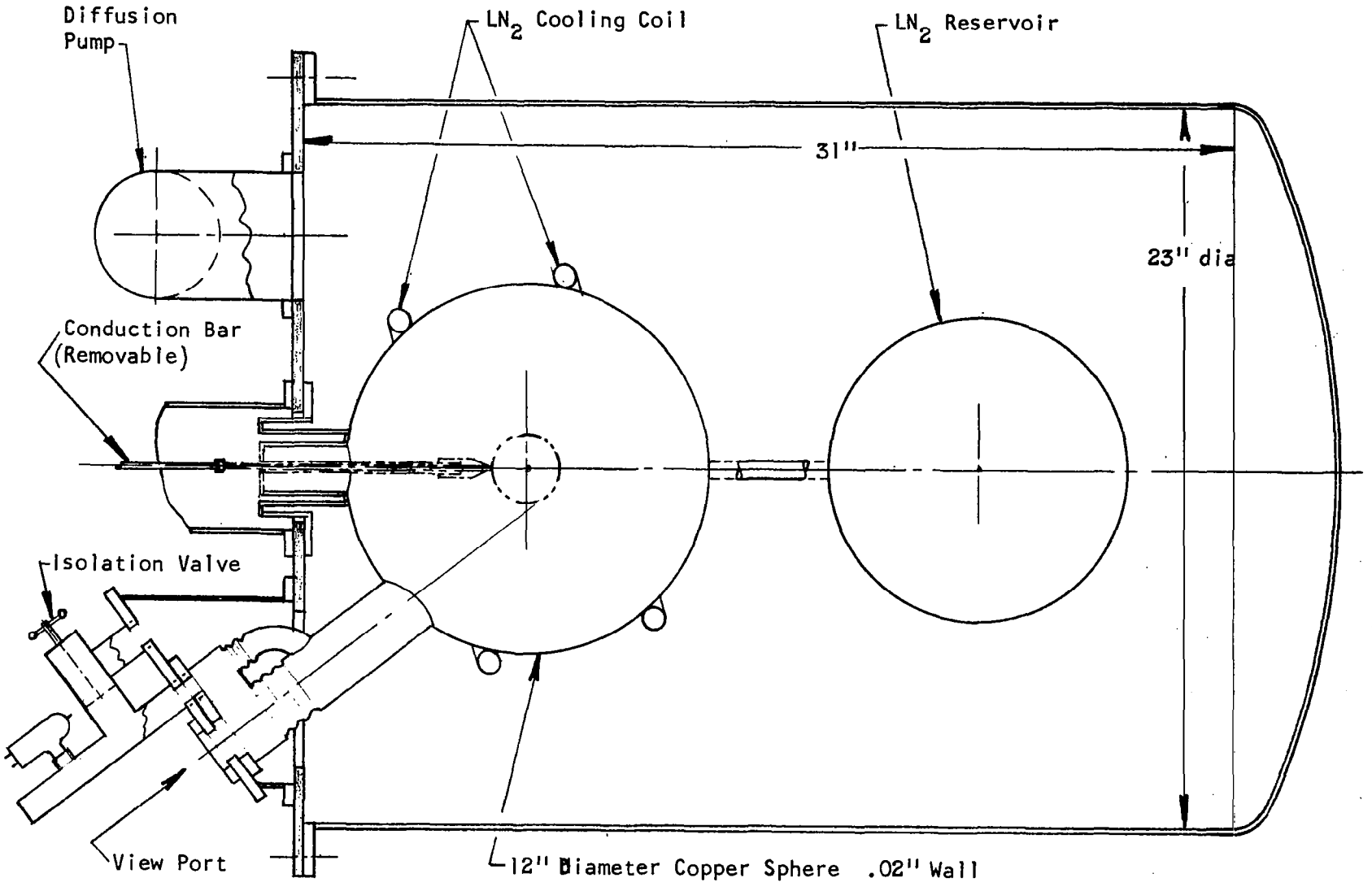

Fig. 1. Facility Schematic

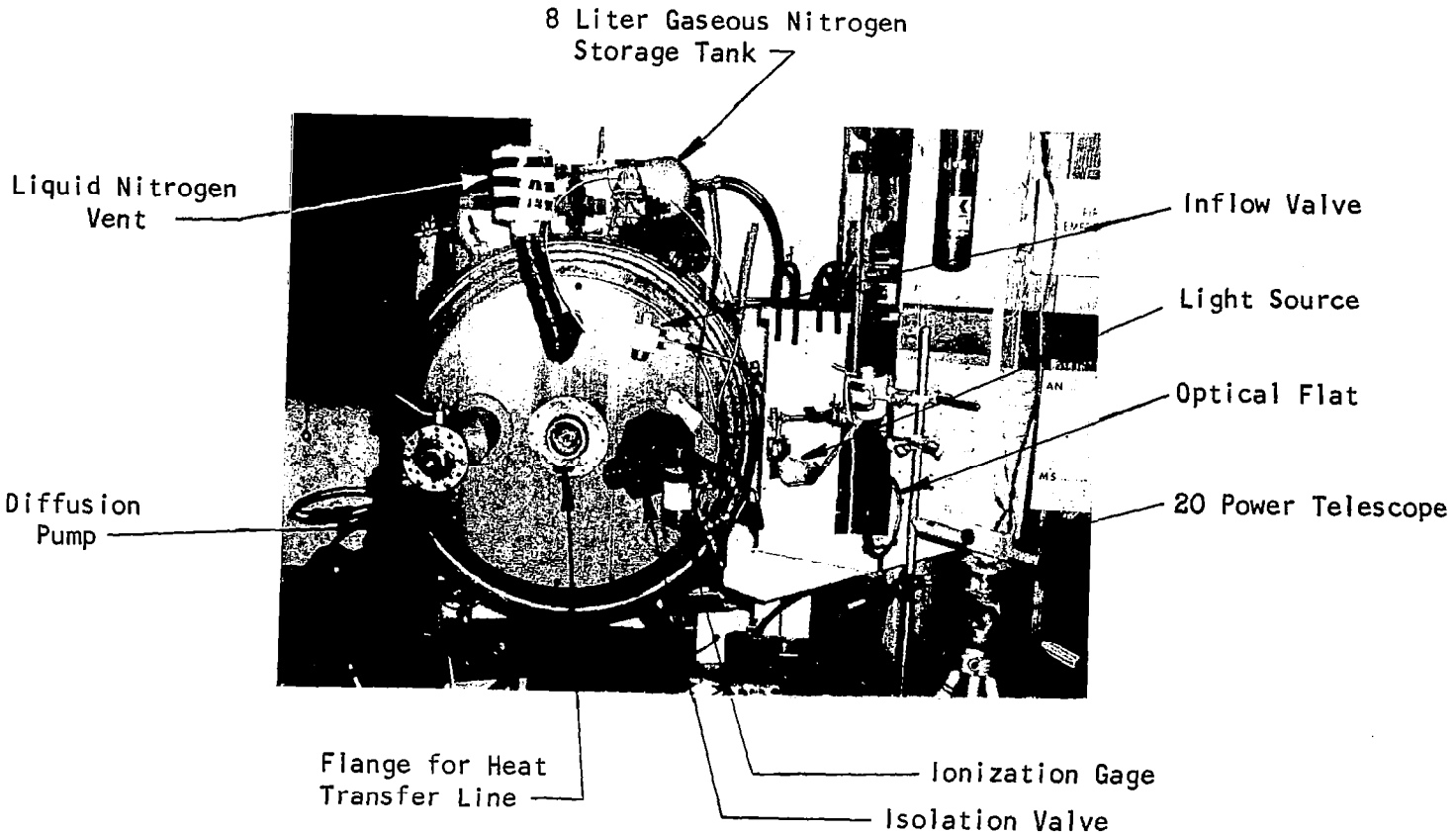

Fig. 2. Experimental Layout

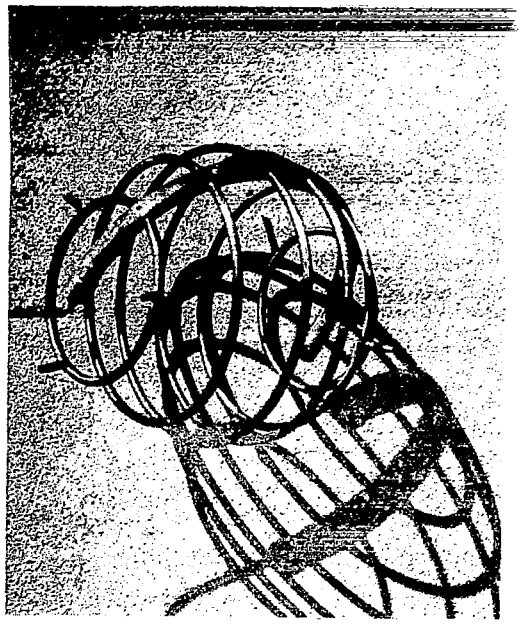

(a) Gas Manifold

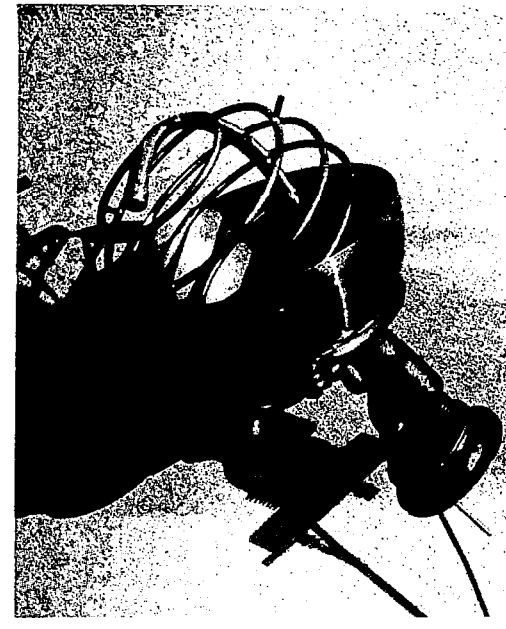

(b) Sphere Subassembly

(c) Sphere Subassembly

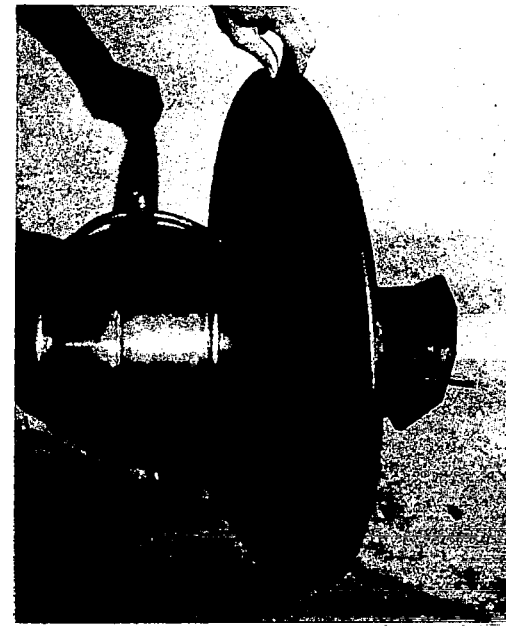

(d) Sphere Assembly

Fig. 3. Assembly and Mounting of the 12" Sphere

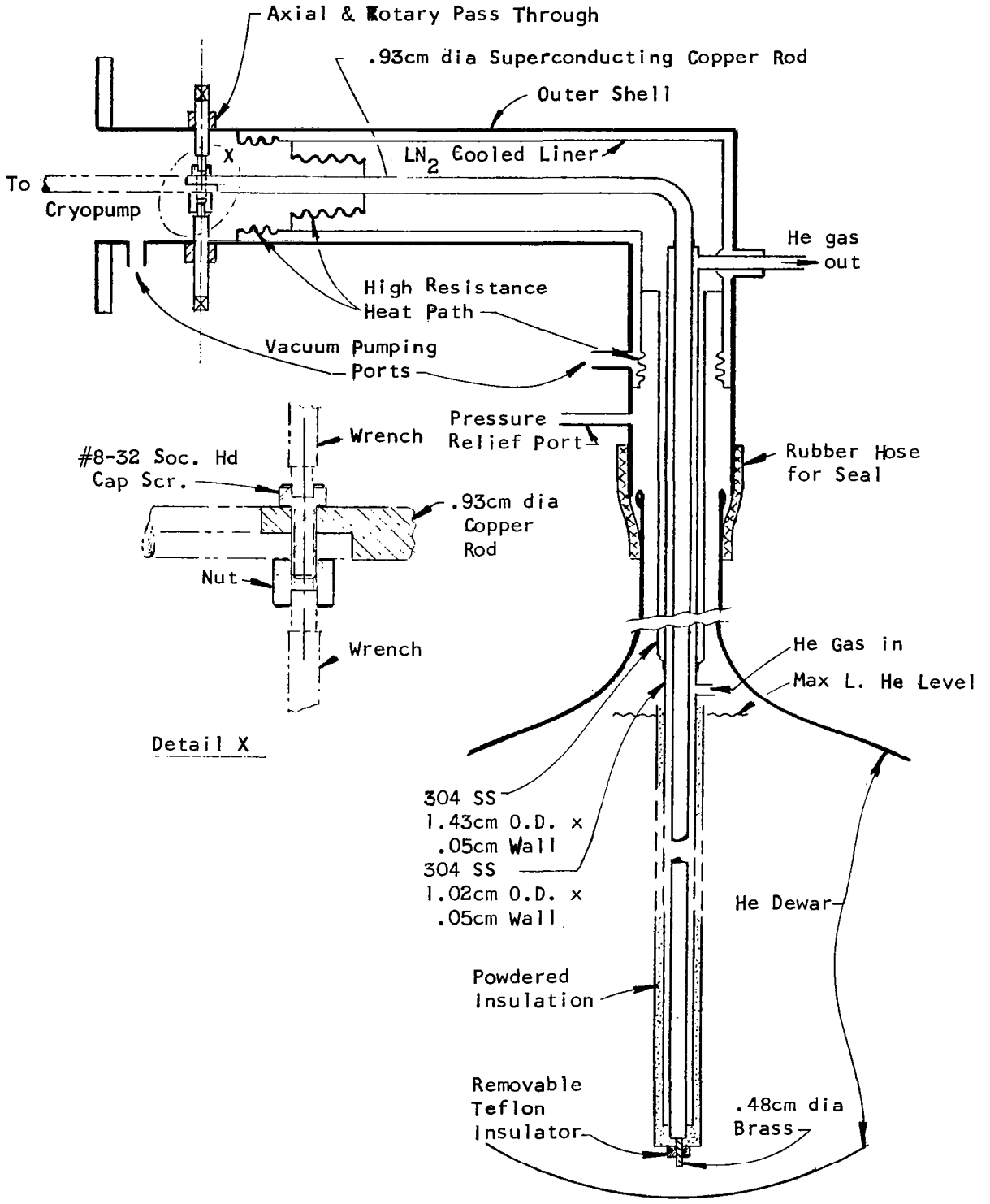

Fig. 4. Heat Transfer Line

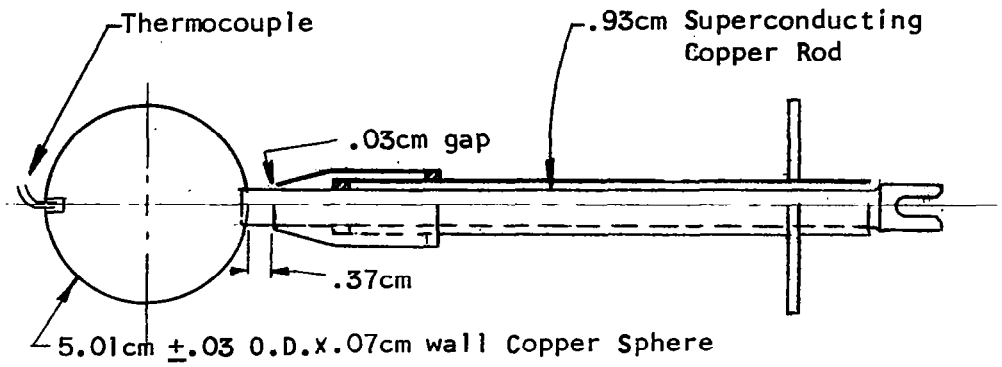

Fig. 5. Spherical Cryopump

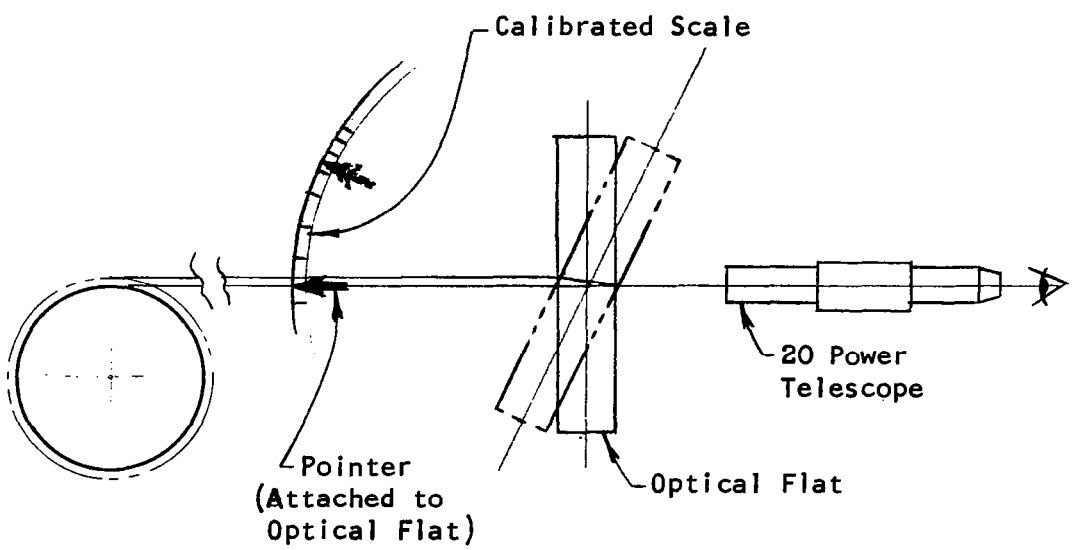

Fig. 6. Optical System For Measuring the Thickness of the Condensate Layer

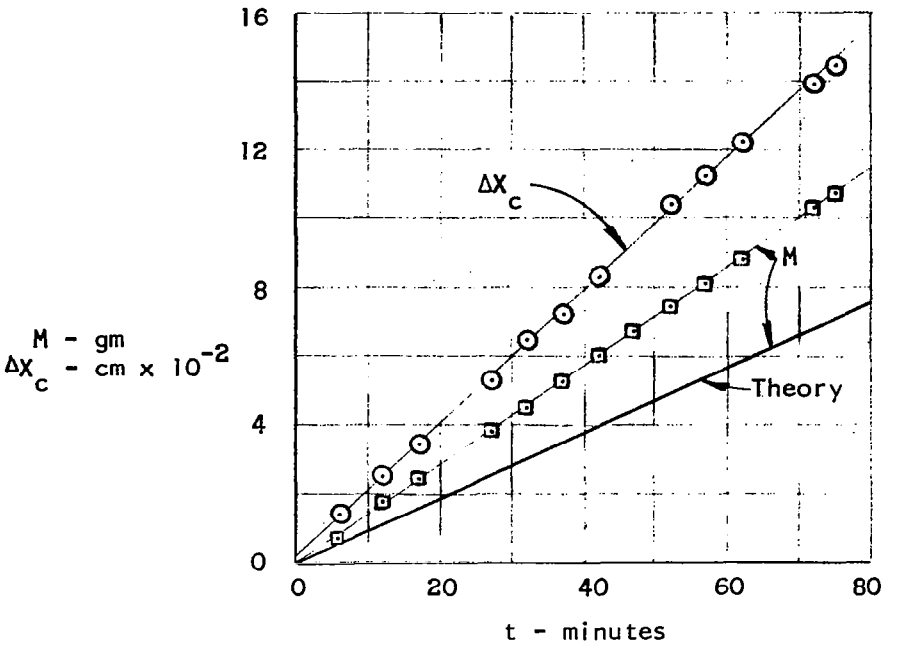

Fig. 7. Variation of M and ΔX_c with Time (P = 10^{-3} torr)

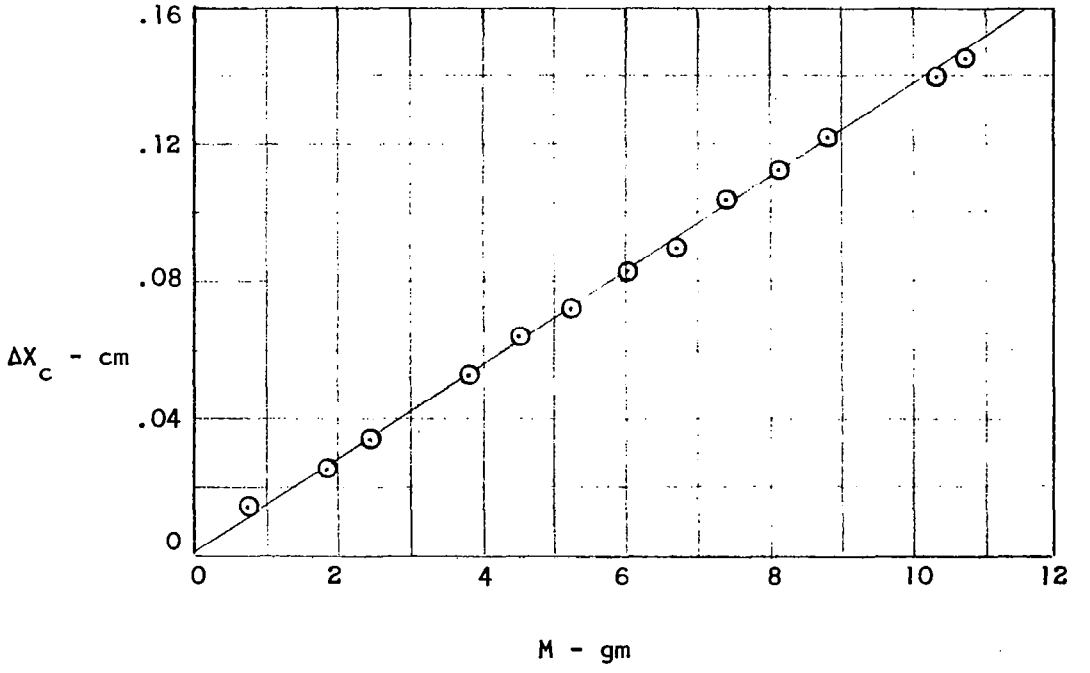

Fig. 8. ΔX_c versus M (P = 10^{-3} torr)

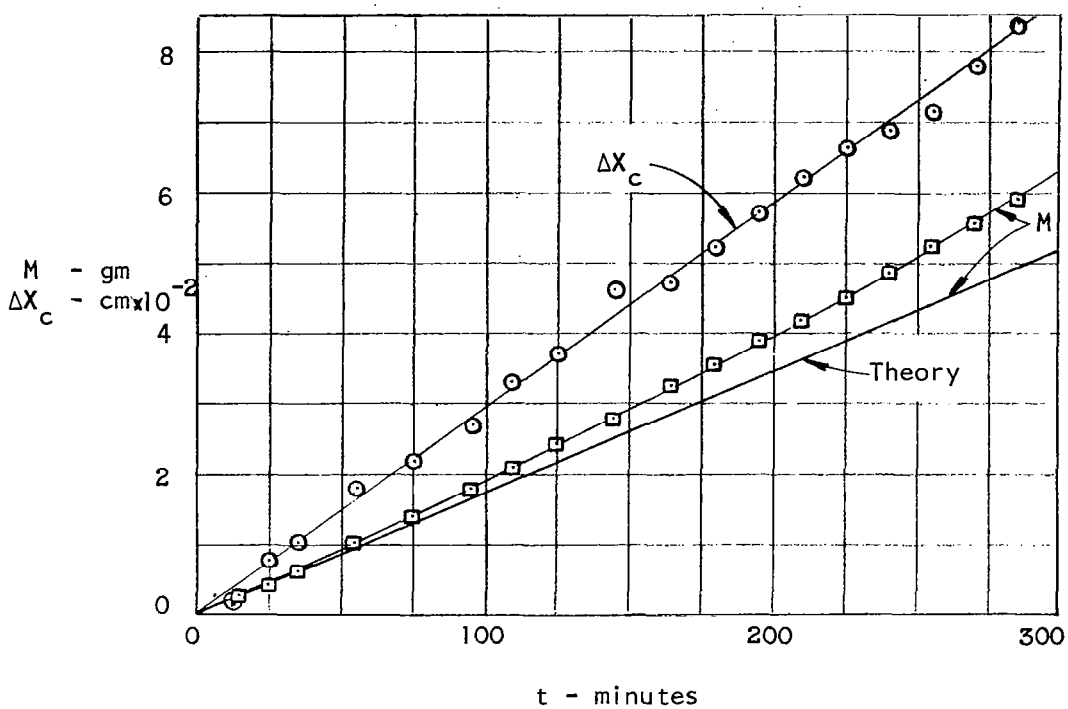

Fig. 9. Variations of M and ΔX_c with Time ($P = 2 \times 10^{-4}$ torr)

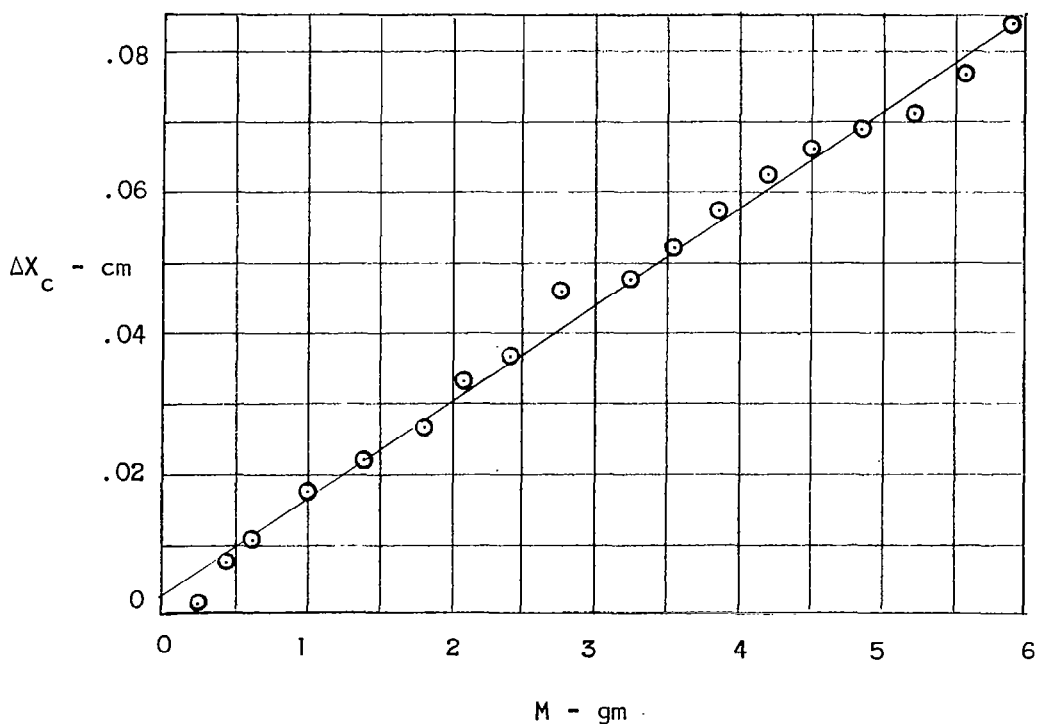

Fig. 10. ΔX_c versus M ($P = 2 \times 10^{-4}$ torr)

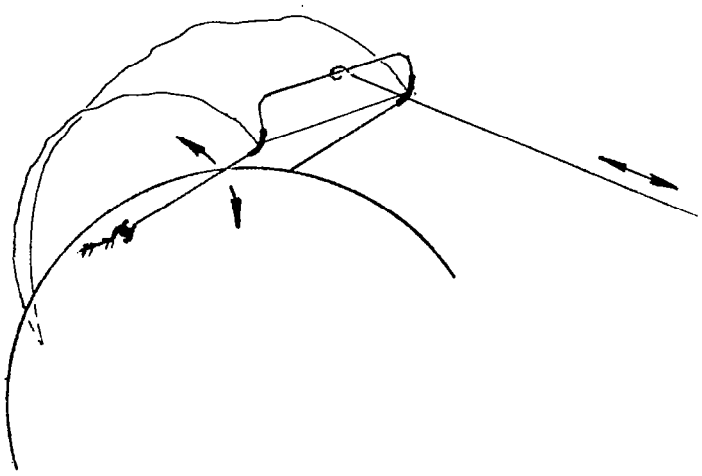

(a) Assembly

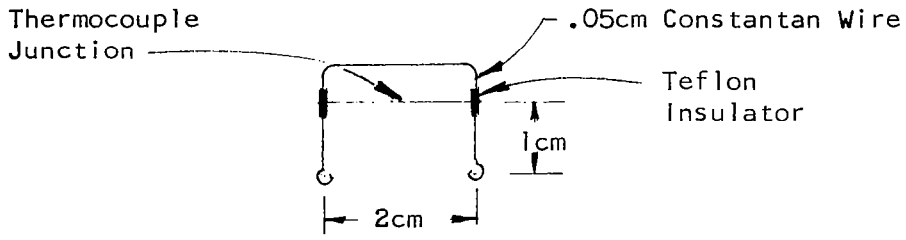

(b) Support Detail

Fig. 11. Movable Thermocouple

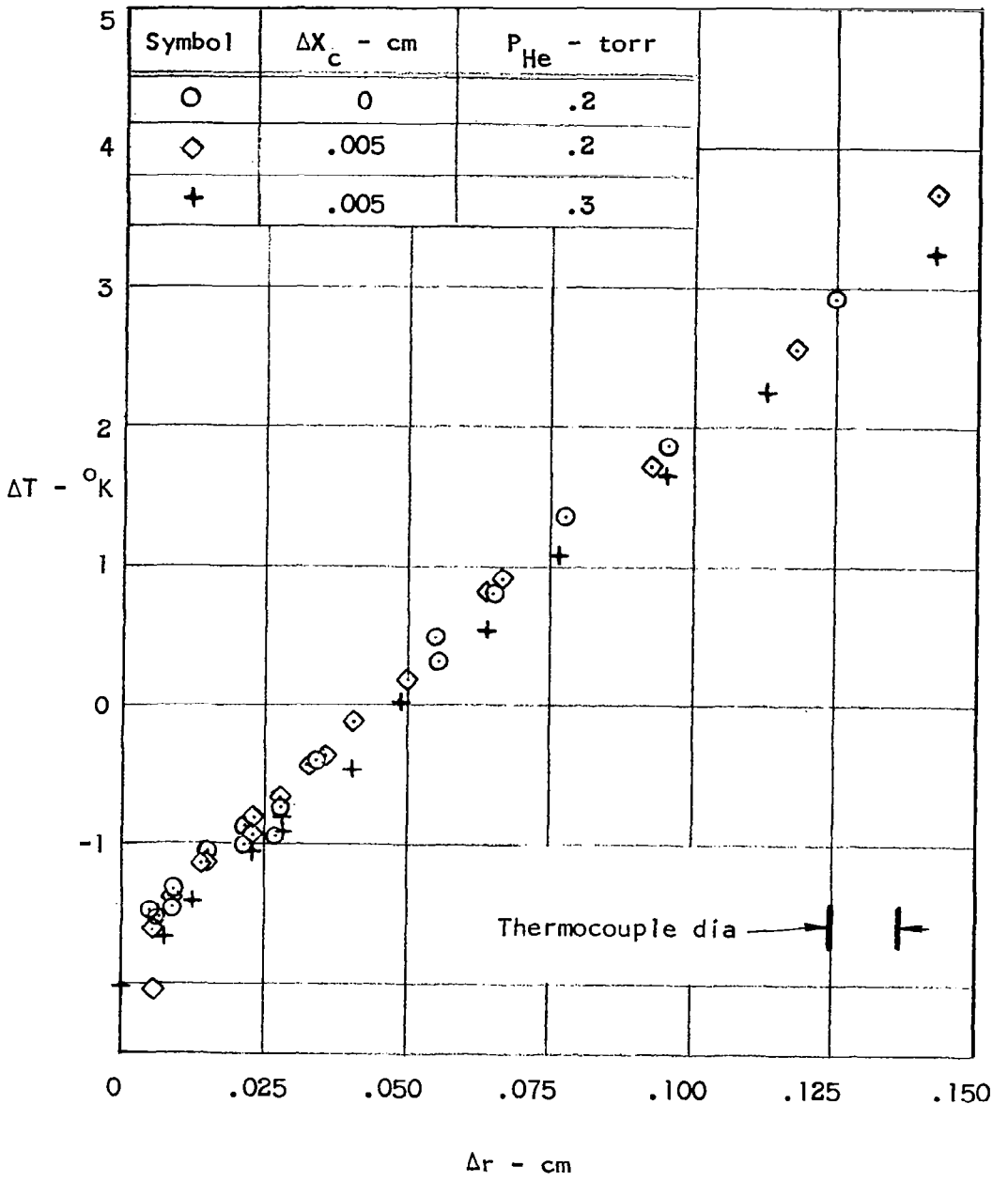

Fig. 12. Helium Temperature Profiles (T_w - 25°K)

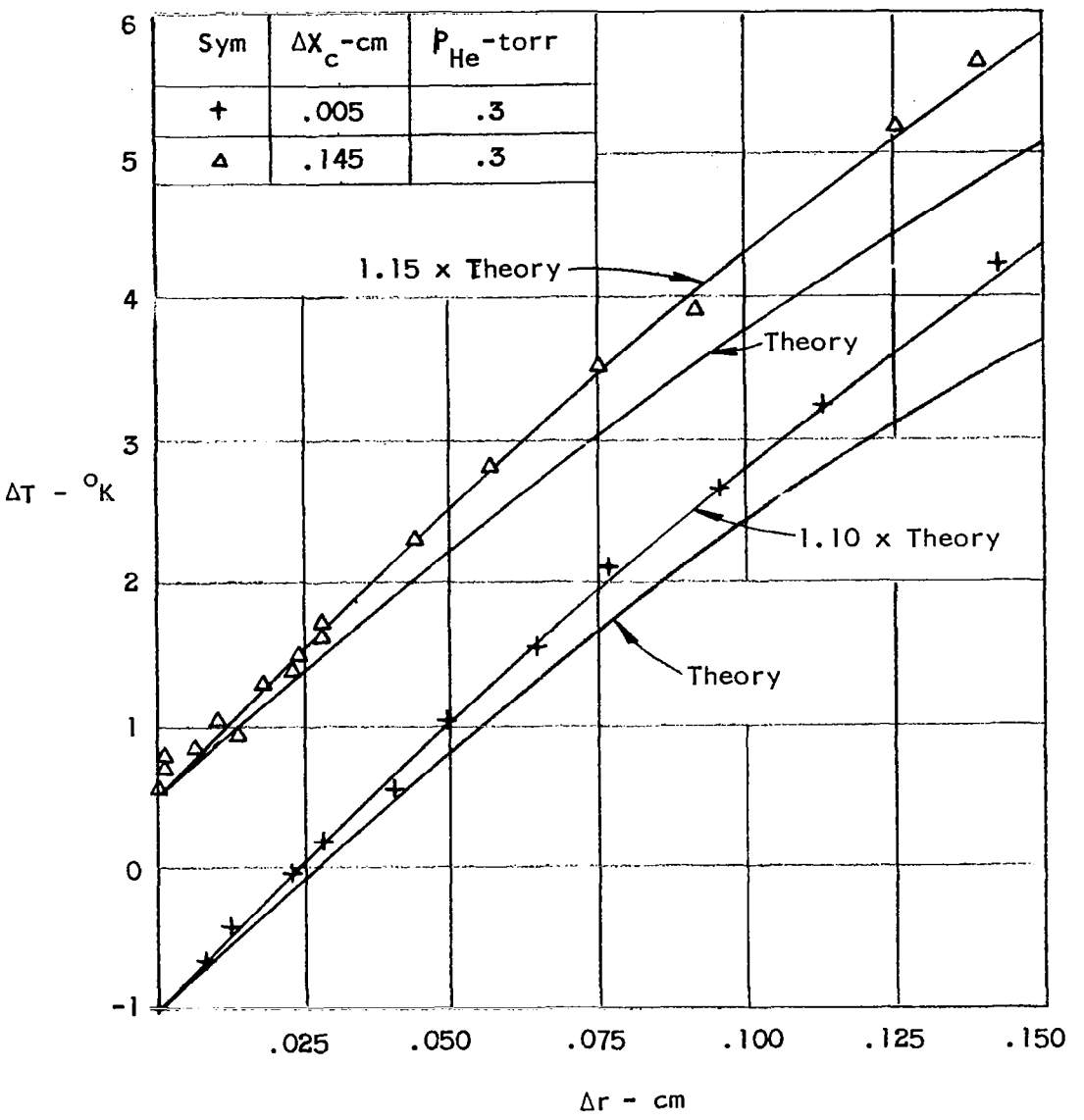

Fig. 13. Helium Temperature Profiles
($T_w = 25^{\circ}K$, $P = 10^{-3}$ torr)

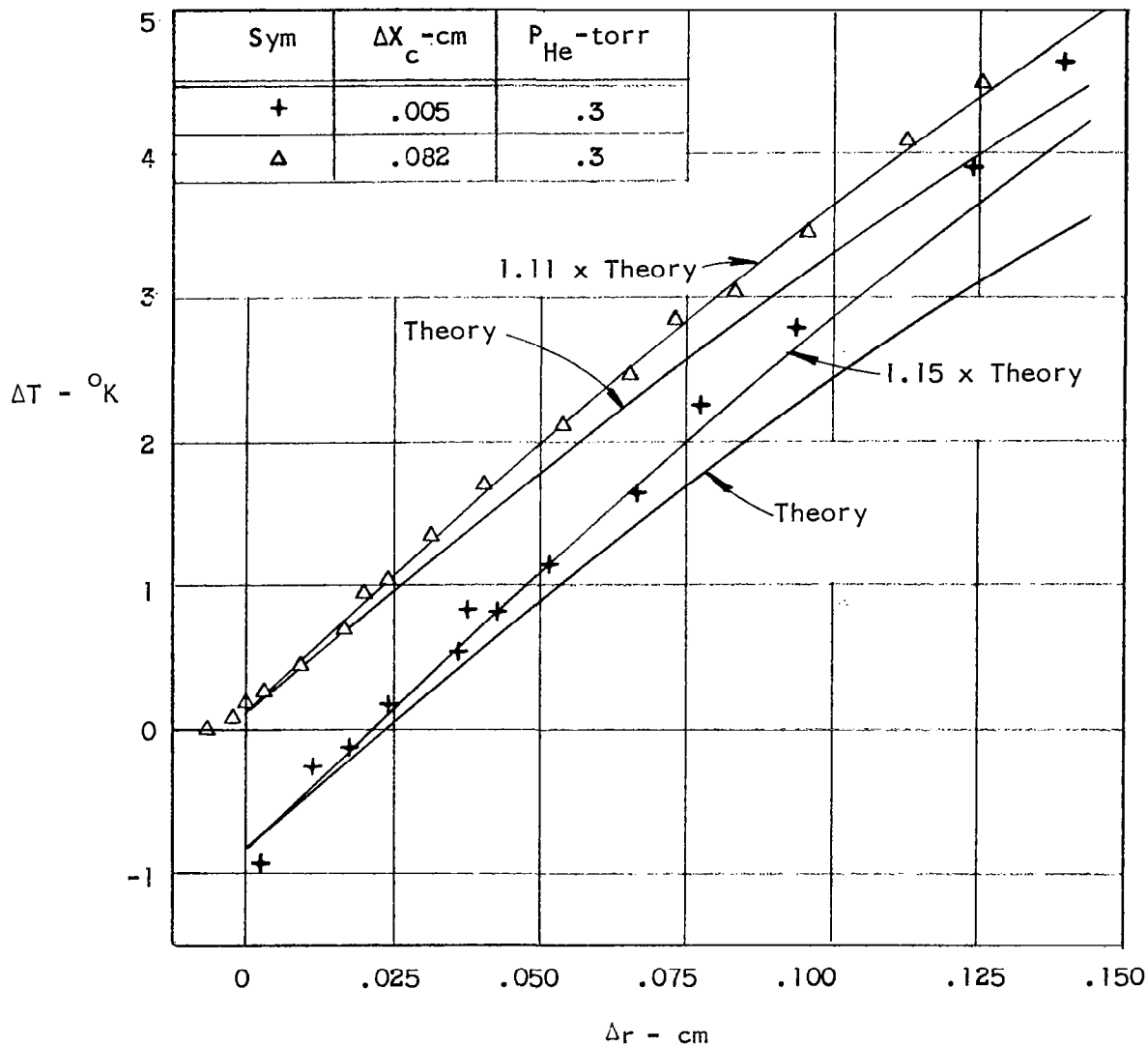

Fig. 14. Helium Temperature Profiles ($T_w = 26^{\circ}K$, $P = 2 \times 10^{-4}$ torr)

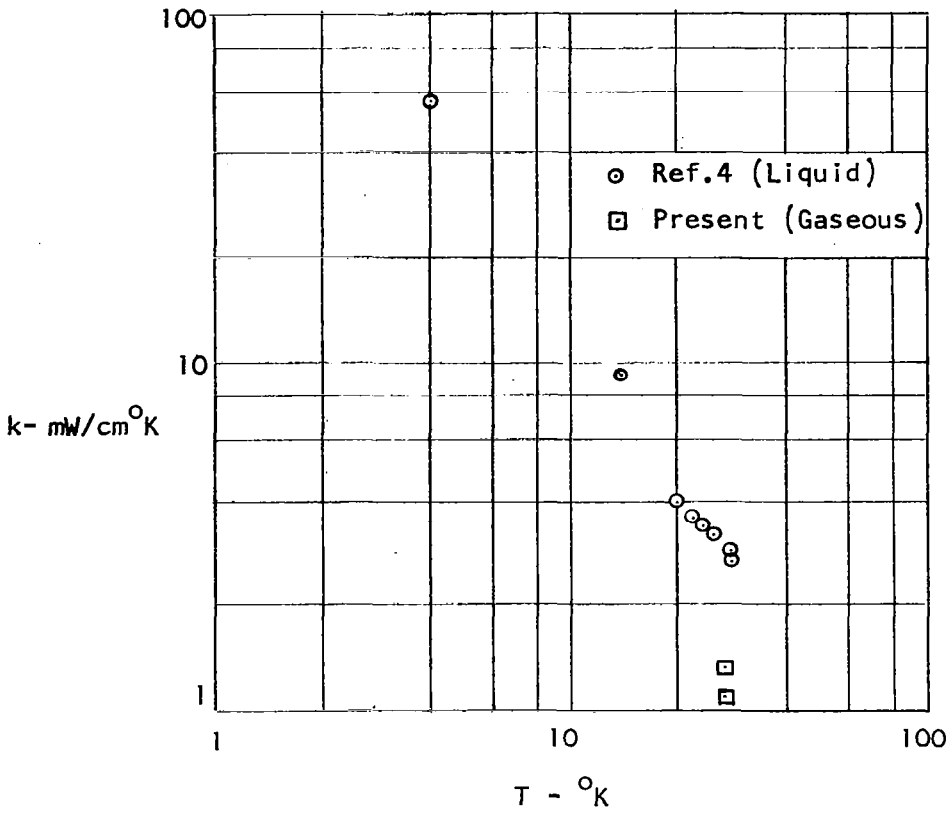

Fig. 15. Thermal Conductivity of Solid Nitrogen Formed From Liquid and Gaseous States

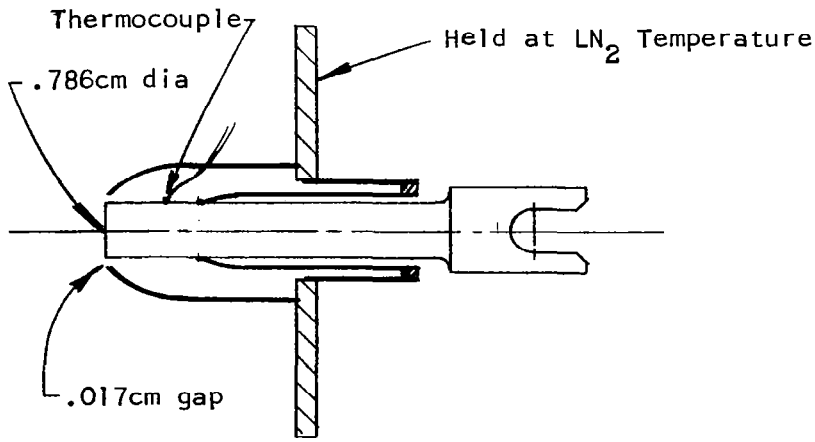

Fig. 16. Disc Cryopump

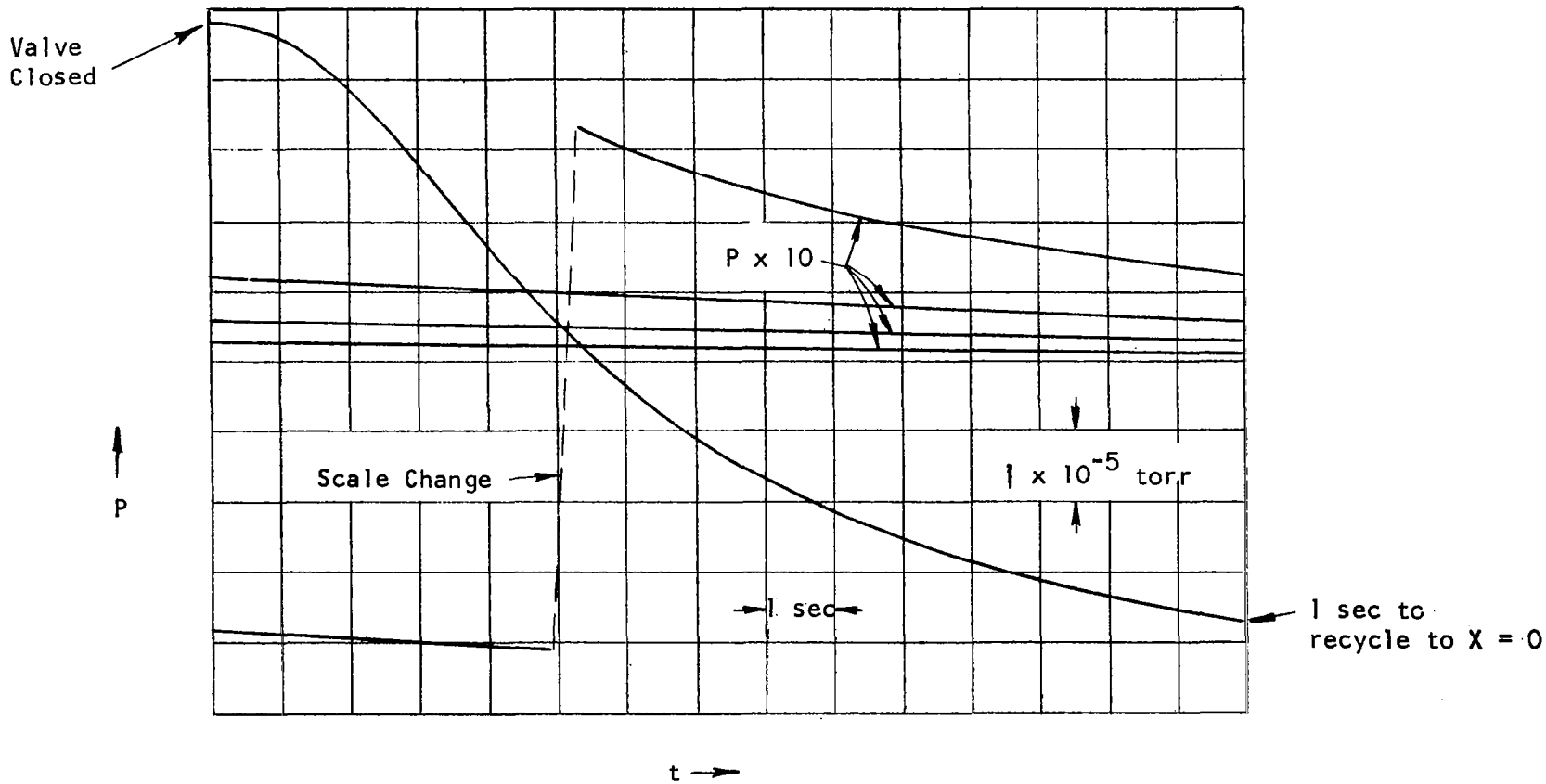

Fig. 17. Typical Data Obtained From X-Y Plotter

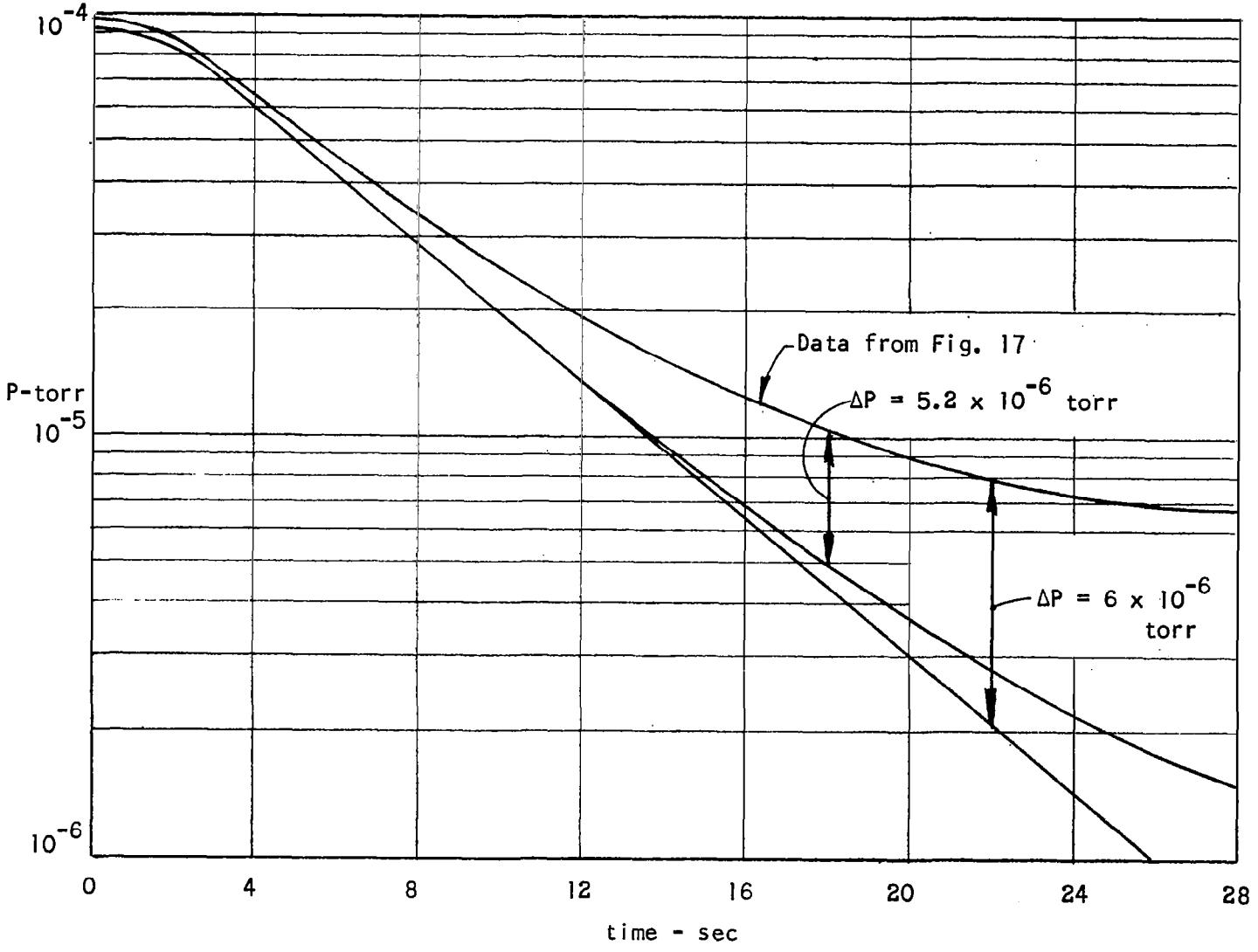

Fig. 18. Pumpdown Curve Corrected for Final Pressure

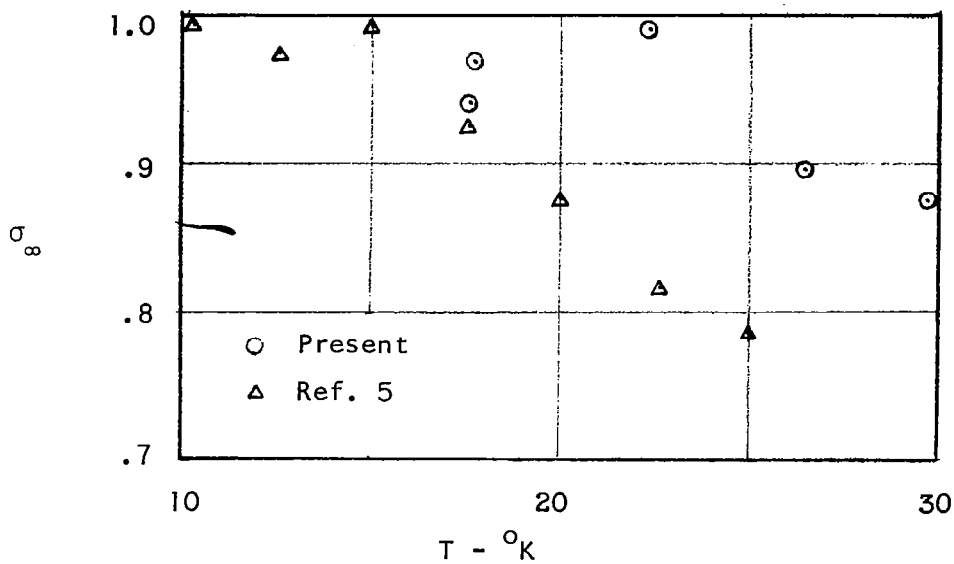

Fig. 19. Variation of Sticking Coefficient With Cryopump Temperature

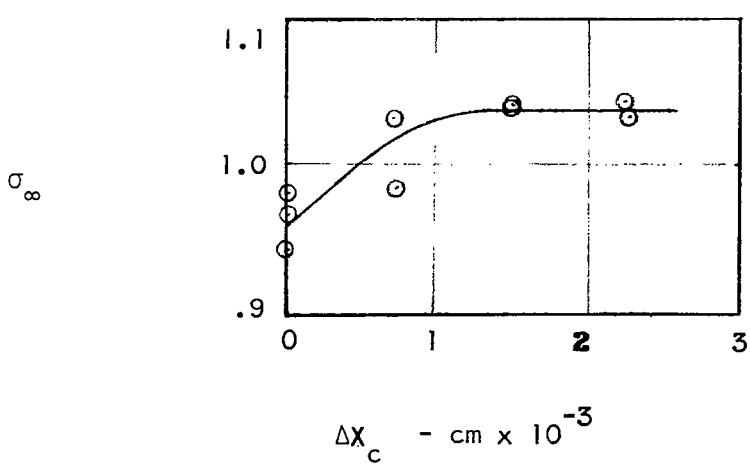

Fig. 20. Variation of Sticking Coefficient With Condensate Thickness

NASA-Langley, 1966

"The aeronautical and space activities of the United States shall be conducted so as to contribute . . . to the expansion of human knowledge of phenomena in the atmosphere and space. The Administration shall provide for the widest practicable and appropriate dissemination of information concerning its activities and the results thereof."

—NATIONAL AERONAUTICS AND SPACE ACT OF 1958

NASA SCIENTIFIC AND TECHNICAL PUBLICATIONS

TECHNICAL REPORTS: Scientific and technical information considered important, complete, and a lasting contribution to existing knowledge.

TECHNICAL NOTES: Information less broad in scope but nevertheless of importance as a contribution to existing knowledge.

TECHNICAL MEMORANDUMS: Information receiving limited distribution because of preliminary data, security classification, or other reasons.

CONTRACTOR REPORTS: Technical information generated in connection with a NASA contract or grant and released under NASA auspices.

TECHNICAL TRANSLATIONS: Information published in a foreign language considered to merit NASA distribution in English.

TECHNICAL REPRINTS: Information derived from NASA activities and initially published in the form of journal articles.

SPECIAL PUBLICATIONS: Information derived from or of value to NASA activities but not necessarily reporting the results of individual NASA-programmed scientific efforts. Publications include conference proceedings, monographs, data compilations, handbooks, sourcebooks, and special bibliographies.

Details on the availability of these publications may be obtained from:

SCIENTIFIC AND TECHNICAL INFORMATION DIVISION

NATIONAL AERONAUTICS AND SPACE ADMINISTRATION

Washington, D.C. 20546